Australian Journal of Basic and Applied Sciences, 3(1): 254-266, 2009
ISSN 1991-8178

Use of Remote Sensing and Geological Studies in the Exploration for Iron Deposits in the Oweinat, El Dakhla District, Western Desert, Egypt.

[1]Ramadan, T.M., [1]EL Kelani, A.H., [2]Hassaan, M.M. and [1]Salem, M.S.

[1]National Authority for Remote Sensing and Space Sciences, Cairo, Egypt.
[2]Al Azhar Univ., Faculty of Sciences, Geology Dept.

Abstract: This study deals with the iron deposits and occurrences in the the south western part of the Western Desert in the Arab Republic of Egypt. This district is mainly covered by Paleozoic, Mesozoic and Quaternary sediments. Volcanic sheets, dykes and plugs are cutting the Paleozoic and Mesozoic sediments. The stratigraphic succession of the Dakhla basin includes the following formation: the Gilf (Carboniferous), Abu Ras (Permo-Triassic), Abu Ballas (Late Jurassic – Early Cretaceous), El Burg (Albian – Early Cenomanian) and Taref (Late Cretaceous). Polyphases basaltic flows were recorded and they are of Carboniferous, Cretaceous and Tertiary ages. Fieldwork and mineralogical studies indicate that the highest concentrations of iron oxides are found in the exposures of El Burg Formation that are located near BIF-bearing gneisses of Archean age. Furthermore, all highly ferruginated sections in the studied district occur between Lat. 23° and 24° 30' N. The increase of iron oxides concentrations to the northeast follows the trend of the Precambrian Pelusium Megashear Zone. The existence of the El Burg Formation is probably related to grabens and micro basins. It seems that the faults and basalt flows cutting mainly the El Burg Formation control the distribution of iron deposits. Moreover, a recorded magnetic anomaly in the Gilf El Kebir area coincides with stratigraphic successions hosting iron-oxide-bearing beds, displaying thicknesses about 2 m each. These observations suggested that areas covered by the El Burg Formation, located in the area between Lats. 23° 00'– 24° 30' N and transected by basalt flows and faults, are the most promising for further geologic exploration for iron deposits.

Key words: Remote-sensing, geochemical, Western Desert, iron deposits, Egypt.

INTRODUCTION

The study district lies at the southwestern part of the Arab Republic of Egypt, between Lat. 23° 00' -25° 00' N and Long. 25° 15'- 29° 45' E (Fig. 1). This district includes Paleozoic, Mesozoic and Quaternary sediments, unconformably overlying Archean – Proterozoic basement rocks outcropping in the south western part of the district. Due to its inaccessibility, very few authors described the geology of the study area (e. g. Dardir, 1981, Issawi, 1982, El Ghawaby, 1984, El Kelani, 1992 and Issawi, 1996). In 1981, four samples from the Black Hill region were chemically analyzed in the EGSMA Lab., in which Fe_2O_3 content ranging from 58.3 to 15.1 %, MnO content from 12 % to 0.15 % and CaO contents from 2.59 to 1.19 % were found (Dardir, 1981). El Ghawaby, (1984), mentioned that the deformed Precambrian terrain in the Gilf El Kebir area was subjected to epiorogenic movement in Paleozoic and Mesozoic times, during which gravity faults have developed and generated positive and negative topographic features with deltaic deposition during the Paleozoic. A transgression at the end of the Mesozoic (Late Cretaceous) allowed accumulation of calcareous oozes. The opening of the Red sea, rejuvenated the NW-SE gravity faults. These movements were followed by the generation of N-S wrench faults. Issawi, *et al.* (1996) reviewed the available literatures on the stratigraphy of the Phanerozoic of Egypt in order to understand the geodynamics that controlled the syn- and post-depositional geologic history of the region. Mineral exploration can be more efficiently performed by an integrated approach based on remote sensing and GIS techniques (Bhattacharya *et al.*, 1993; Venkataraman *et al.*, 1997 and Ramadan and Sultan, 2004).

Corresponding Author: Talaat Ramadan, National Authority for Remote Sensing and Space Sciences, Cairo, Egypt.

This article aims at developing and implementing methodologies for using Landsat ETM+ and Radarsat in exploration for iron ore deposits in the southwestern part of the Western Desert. Moreover, the results of airborne magnetic study given by Ramadan and Sultan, (in press) were used. Field studies were carried out to verify the obtained results.

MATERIALS AND METHODS

The use of spatial integration of various data sets including Landsat ETM+ and Radarsat images and the geological maps of scale 1: 50,000 in exploration for iron ores in the studied district form the essential objective of this work. Landsat ETM+ and Radarsat images were processed at the National Authority for Remote Sensing and Space Sciences (NARSS) Image Processing Lab, using the ERDAS Imagine-8.8 software on Sun Spark workstation. Six scenes (Path 179 , Raw 44, Path 179, Raw 43, Path 178 , Raw 44, Path 178, Raw 43, Path 177 , Raw 44, Path 177, Raw 43, Date 2003) covering the investigated area, have been geometrically corrected and radiometrically balanced. False colour composite images (bands 7, 4, 2 in RGB) for the studied district were used to discriminate Phanerozoic sediments from surfaces covered by sand dunes and sand sheets.

Different density slices technique was also used to create an iron index map, using band-ratio 3/1. This technique converts the 256 shades of gray in an image into discrete intervals, each corresponding to a specific range of digital numbers (DN). Different density slices are shown as separate colors that can be draped over background images. According to Sabins (1997) Landsat TM band-ratio 3/1 is produced by dividing the digital number (DN) of one band by another to yield an image that enhances spectral differences and reduce the morphology effect. Landsat ETM+ band-ratio 3/1 is used because iron minerals have reflectance and absorption features in these bands, respectively. The second set of the images (Radarsat-1) was acquired on Sep. 16, 1998 and covered most of the study area. These images were acquired from the Standard Beam 5, which features a swath width of 100 km, spatial resolution 25 m and incidence angle of 39˚ at the scene centre. Twenty two stratigraphic sections were measured and studied in the studied region. New geological and stuctral maps for the study area were prepared using Landsat TM images and field study. Moreover, 15 representative samples from the ferruginated beds of the Gilf El Kebir Plateau were mineraliogically studied and analyzed for major oxides at the Egyptian Geological Survey (EGSMA).

RESULTS AND DISCUSSION

General geologic setting:

The study area is located within the Dakhla basin. This basin is flanked to the south by many basement outcrops at Gabal Oweinat and Gabal Kamil, to the west by the Oweinat-Bahariya (UBP) arch, whereas it is flanked to the east by the Tarfawi-Qena-South Sinai (TQS) arch (Fig. 2). This basin is traversed by the NE Pleusium megashear zone. Use of the aeromagnetic map of Egypt (Aero Service Division, Western Atlas International, INC., Huston, Texas) enabled to modify the boundary of the Dakhla Basin suggested by Hermina and Issawi, (1994, Fig. 2).

The lower Mesozoic part of studied exposures were situated in a wide tract of Gondwana surface away from areas covered by glaciogenic deposits. It seems that North Africa including Egypt was located in subtropical to tropical zones most probably uncovered by water due to a major uplift of this part of east Gondwana and also due to a low sea level coinciding with the glacial event (Hamilton and Krinsley 1967; Reed and Watson 1975). The deposits of interest for the present study are 30 to 40 m thick conglomerates on top of the Gilf Formation. All authors agree that the Abu Ballas Formation was initially deposited in braided streams gradually changing with time to deltaic and marshy environments that ended by development of a shallow sea. The El Burg Formation represents the second sedimentary cycle in the Cretaceous history of south Egypt where fluviatile and deltaic sediments dominate at the base of the sequence and marine incursions onlap these continental sediments.

The Landsat ETM+ image band 1 and bands (7,4,2 in R,G,B) for the study area exhibits three characteristic geomorphological features:

1- Three parallel ridges (R1, R2 and R3, Fig. 2).
2- Several wadis filled with sand sheets trending NE-SW, separating the El Gilf El Kebir plateau from the Abu Ras plateau (Fig. 2).

3- Several wadis filled with sand dunes and sand sheets trending NNW-SSE, separating the El Gilf El Kebir plateau from the Abu Ballas plateau with apparent displacement of the three ridges (Fig. 3a).

Landsat ETM+ ratio image (5/7,5/1,4 in R,G,B) distinguished between the Abu Ras Formation (yellow colour), the El Burg Formation (Red colour), the wadi deposits (light green) and the sand sheets (blue colour), (Fig. 3b). The density slices band ratio 3/1 (Fig. 3c) shows presence of widespread purple, colour which indicates high ferrugination.

In this respect, the Radarsat image revealed some subsurface features underneath the recent sands, filling the above mentioned wadis as follows:

1. A NE-SW subsurface fault separated the Abu Ras Plateau from the El Gilf El Kebir Plateau. This fault records continuous rejuvenation of the NE Precambrian Pleusium megashear zone.
2. The existence of a subsurface major fault trending NNW-SSE underneath the recent sands filling the wadi, separating the Gilf El Kebir Plateau from the Abu Ballas Plateau (Fig. 3d). This fault caused a northward displacement of the three ridges (Dashed line (Fig. 3d).

Existence of some bed rocks bearing iron oxides, beneath the recent sands, east of El Gilf El Kebir Plateau (B1,B2,B3 - Fig. 3d).

Stratigraphy of the study region:

The measured and studied 22 stratigraphic sections (Fig. 2) enabled establishment of the stratigraphic succession of the Dakhla basin as follows from base to top: the Gilf (Carboniferous), the Abu Ras (Permo-Triassic), the Abu Ballas (Late Jurassic-Early Cretaceous), the El Burg (Albian – Early Cenomanian) and the Taref (Late Cretaceous) formations (Fig. 4). The composite stratigraphic section of the studied district is shown in Figure (5).

Volcanic rocks occur in the study area covering various formations (Fig. 6). These volcanics include basalts (black in colour), trachytes (green or grey in colour) and phonolites of green colour. The basaltic dykes are ranging in thickness from 1 to 2 m and in length from 1 to 2 km. They trend NE-SW and NW-SE. The basalt sheets in this region cover many patches of the El Burg Formation. The basaltic dykes and / or sills also cut or cover the El Burg Formation. Some eruptions took place through fissures around the vents producing dykes of different areal extension and frequently, form cinder cones. The volcanic cinder cones transect by the El Burg and are covered with the Taref and the Dakhla formations.

These volcanic eruptions, the surrounding rocks exhibit several characteristics as dykes of hardened sandstone, quartzitic sandstone, highly ferruginated quartzitic sandstone. Several volcanic flow sheets cover the El Burg Formation especially in the Double Peak area (Lat. 23° 58'N and Long. 29° 35'E).

The El Burg Formation especially at Nusb El Balgum area consists of sandstones and clays. Composite plugs with basalt at the core of the plug and trachyte at the outer rim are observed through the area. Different plugs of the same composition follow a NE trending fault, which means that the plugs are controlled by structures prevailing in the investigated area.

Different authors (Andrew 1937, El Meneisy and El Kaluoby 1979 and Kamel *et al.,* 1982 and Franz *et al.,* 1987) dated various basalts from the southern part of the Western Desert as ranging from 233 ± 9, 240 + 7 82 and to 32 m.y. These suggests Triassic, Cretaceous and Tertiary ages. Androw (1937), mentioned that some basalts are of Carboniferous age.

Distribution of iron and manganese in the stratigraphic rock units:

The results of the analyzed samples from the area west of the Black Hill, given by Issawi, (1978) show that Fe_2O_3 content ranges from 62.7 to 22.99 %, MnO content from 22.29 % to 0.08 % and CaO content from 8.75 to 1.48 %. Meanwhile, four chemical analyses from the Black Hill region given by Dardir (1981), show that Fe content ranges from 58.3 to 15.1 %, Mn content from 12 % to 0.15 % and CaO content from 2.59 to 1.1.9 %. The study of ferrugination intensity of the Paleozoic-Mesozoic formations in the Dakhla basin and its comparative latitudinal and longitudinal variations in each formation are considered. The intensive ferrugination as well as the chemical analyses for iron oxides content suggest that the studied region is a promising target for detailed exploration for iron deposits, based on the following results:

a. The Gilf Formation in the area between Lat. 23° 55'N - 24° 25' N and Long 29° 03' consists of medium-grained sandstone beds, occasionally colored by limonitic yellow- hematitic reddish brown and glauconitic - manganese violet to black colors. The thickness of these beds is 7- 8 m and 4 - 17.5 m respectively.
b. The Abu Ras Formation in the area between Lat. 24 05' - 24 25' and Long. 24 03' E consists of medium to coarse- grained, brown to dark brown and highly ferruginated sandstones (section A3, Fig. 2). The formation exhibits fining upward and become multicolored mudstones and kaolinitic sandstones. In the studied sections a paleosol horizon overlies most sandstone beds. There are parallel horizons of variable reddish brown colouration due to the variation of the concentration of the iron oxides. There is also leza Ganges of less iron oxides concentration. Southeastward, there are highly ferruginated sandstone horizons capping the topmost beds (section A4 Fig. 2). The thickness of these highly ferruginated sandstone horizons reaches up to 2 m. This enhances an increase of the ferrugination intensity of this formation northwestward.
c. The Abu Ballas Formation consists of violet to reddish brown claystone beds. This formation is located between Lat. 23° 38'N - 27° 27' N and Long. 29° 05' E- 29° 49' E. Ferruginous and manganese patches are occasionally recorded in silty-claystone and siltstone beds of the Abu Ballas Formation in the area located between Lat. 24° 06' 45" – 24° 17' 10" N and Long. 27° 03' 07" - 27° 34' 07" E. The middle part of section G4 (4.5 – 5.5 m thick,) is located at the intersection of Lat. 24 ° 06' 45" N and Long. 27 ° 34' 07" E and it is dark red to reddish brown claystone beds, moderately hard and highly ferruginous with manganese oxide patches. In the northwestern part of the study area (deepocentre of the Abu Ballas basin), the formation is highly ferruginated (Fig. 8a). This favors the high degree of ferrugination of Abu Ballas clays with increase of the depth of the Dakhla Basin in the west and in the north. In the southeastern part of the basin, the degree of ferrugination of the beds is weak. The Abu Ballas Formation in the south eastern part of the Dakhla basin, consists mainly of about 40 m of grey, whitish red, violet and brown highly saline shales and claystones. The ferruginous and manganese oxides concentration of the Abu Ballas claystone beds in the eastern and southern sections is low. In the northern and western sections, the lower part of the Abu Ballas Formation is characterized by greenish brown to greenish purple colors due to the presence of glauconite. Anyhow, throughout the succession, there are several thin beds of reddish brown fine-grained hematitic sandstone full of fossil traces and dwarfed fauna (El Kelany 1992).
d. The El Burg Formation (36 m thick, Sec. G1) in the area located between Lat. 23° 00' 15" - 23° 13' 27" N and Long. 27° 17' 36" is ferruginated and characterized by presence of intensively ferruginated sandstone beds (28 m thick). Westward at Long 26° 01' 39", the top beds of total thickness 40 m are moderately ferruginous with manganese oxides (Sec. G2, Fig. 2). Ironstone concretions are occasionally present particularly in the silty beds. Northwestward, at the intersection of Lat. 25° 36' N and Long. 29° 10' 33" E, the sandstone beds of El Burg Formation show weak ferruginous and manganiferous coloration (Sec. G9). The basal sandstone part of the El Burg Formation (45 m thick, Sec. G5) in the area located between Lat. 24° 15' 05" - 24° 29' 22" N and Long. 27° 17' 14" E is ferruginous and bearing manganese oxides. The topmost 2 ms are highly ferruginated. At Long. 27° 51' 45" E, the topmost sandstone part of total thickness 52 m is ferruginated (Sec. G8). The intensity of the ferrugination fluctuates southeastward. The sandstone beds of thickness about 70 m at Long. 27° 51' 45" show weak ferrugination, while, the beds at Long. 29° 12' 44" E are highly ferruginated (Sec. G7, Fig. 8b).

El Kelany (1992) believed that the variation of the ferrugination intensity is most probably related to the stratigraphic position of the formations in relation to folding where the anticlines and synclines form undulations along the course of the major faults in the area.

The cores of the anticlines are mainly occupied by the Abu Ras and Abu Ballas formations, while the cores in the synclines are mainly of the El Burg Formation. In this respect, Issawi (1978) observed presence of closed basins and domes near the course of the major faults. The sandstone beds of the El-Burg Formation that located in the south-eastern part of the Dakhla basin between Lat. 23° 45' – 24° 00' N and Long. 29° 45' - 29° 52' E, show southward decrease in intensity of ferrugination, where the color is violet, brown, grayish and limonitic yellow in a mottling manner (Sec. A 7).

The studied district was part of an airborne magnetic survey conducted over a large segment of the southern and central Western Desert of Egypt by Aero-Service (1985). A total intensity magnetic map for the study area established the magnetic response of each lithologic unit and subsurface faults. It also, recorded the presence of 5 magnetic anomalies (Fig.7 and Table 1).

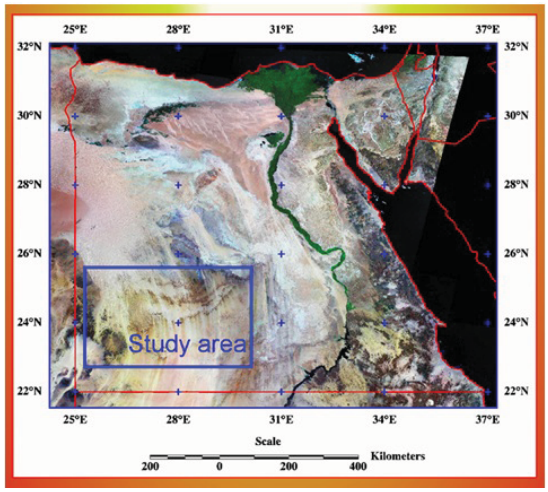

Fig. 1: Landsat ETM false colour image Bands 7,4.2 showing the location of the study district.

The interpretation of this magnetic map resulted in the following results:

a. Separation of the local anomalies of interest at shallow depths from the deep anomalies.
b. High magnetic anomalies with a NE-SW trend are probably related to the basaltic flows and to the iron deposits which are distributed along three ridges.
c. Basement rocks in the northwestern part of the area are at shallow depths and tend to be become deeper in the central part of the Dakhla basin.

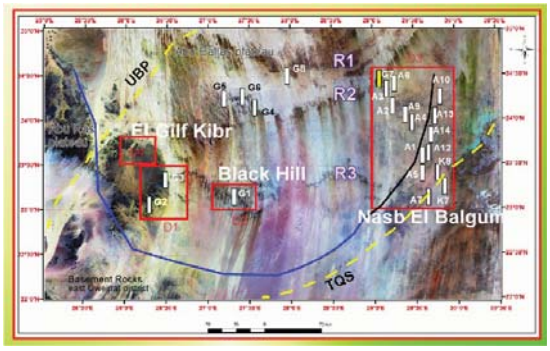

Fig. 2: Landsat ETM+ image showing: the three parallel ridges (R1,R2,R3), the boundary of the Dakhla basin (after Hermina et al., 1961 – yellow dashed line), the boundary of the Dakhla basin (from the processed magnetic data - blue solid line) and the location of the Studied sections (G1 – G8, A1-A9). The studied sites using density slices D1, D2, D3 and D4 indicated by red box.

Results of density slices:

Several sites studied by using density slices D1, D2, D3 and D4 shown in (Fig. 2). The density slices band ratio 3/1 is used for the same the recorded magnetic anomalies **(**Figs. 2 and 7). Chemical analyses for the iron oxides bearing beds in the sections located in the area of the magnetic anomalies No. 1, 6 and 7 will be given to reveal whether the density slices technique is feasible for the iron deposit exploration. Moreover, a site D4 from a region uncovered by airborne magnetic survey also studied. The obtained results as follows:

The iron oxides index map (Fig. 3c) of the magnetic anomaly No.1, (Fig. 7) as well as Nos. 6 and 7 shows presence of widespread purple, colour which indicates high ferrugination. This ferrugination is due to either exposures of ferruginated beds by weathering or washings of fragmented highly ferruginated beds of the Gilf El Kebir Plateau or both. The torques and yellow colors point to moderate and weak ferrugination respectively, most probably due to various degrees of mixing of the weathering products of the highly

ferruginated sand stone beds with eolian sands and the fragments of the barren sandstone beds. Also, the iron oxides index maps of the magnetic anomalies Nos. 6 and 7 (Fig. 7) shows presence of widespread purple, colour which indicates high ferrugination.

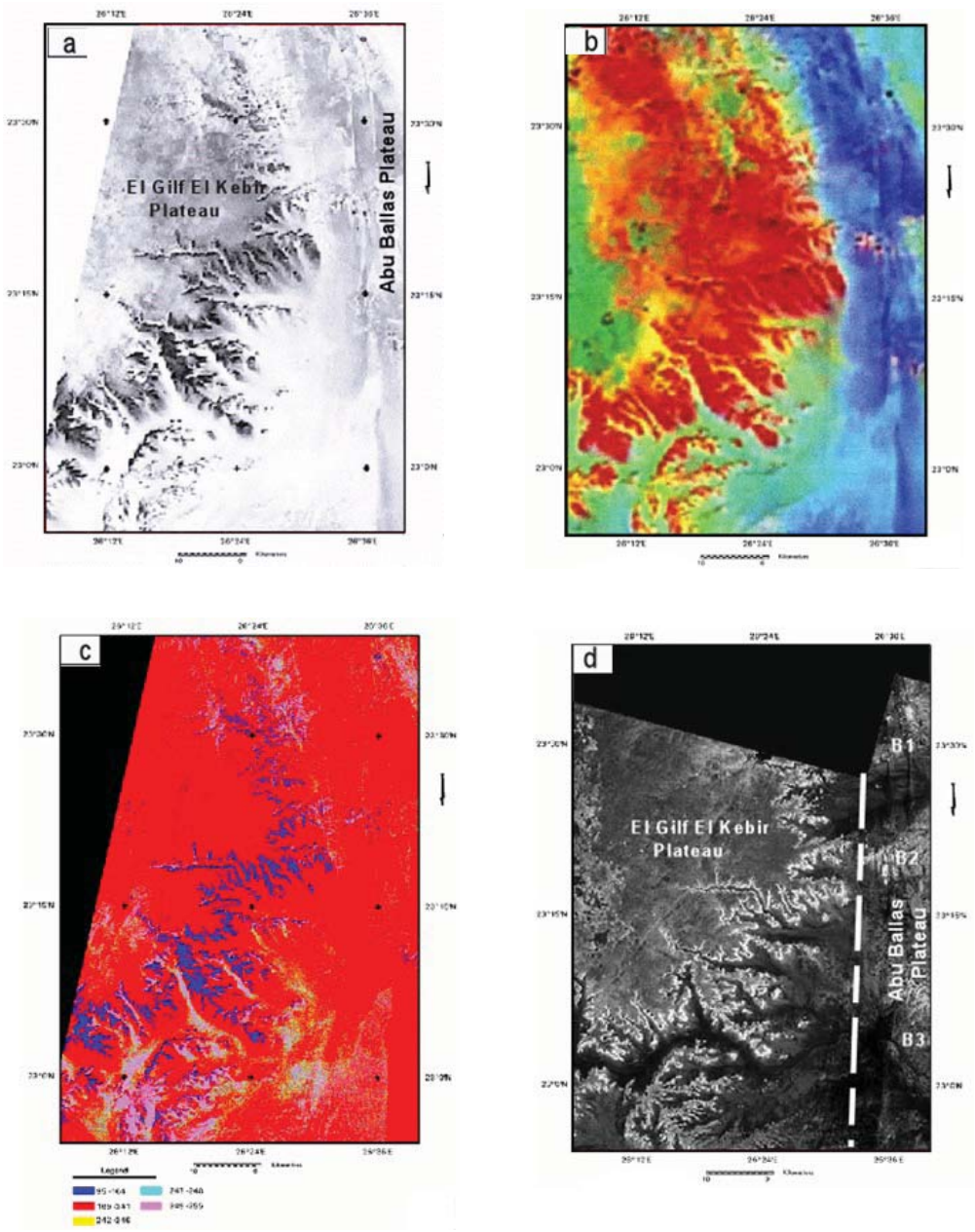

Fig. 3a-d. a: Landsat ETM+ image (band 1) for east of the Gilf El Kebir area. b. Landsat ETM+ ratio image (bands 5/7,5/1,4 in R,G,B) for east of the Gilf El Kebir area. c.Density slices (band ratio 3/1) for east of the Gilf El Kebir area, the highly ferruginated areas are indicated by purple colour. d. Radarsat-1 image for east of The Gilf El Kebir area of the Gilf El Kebir area.

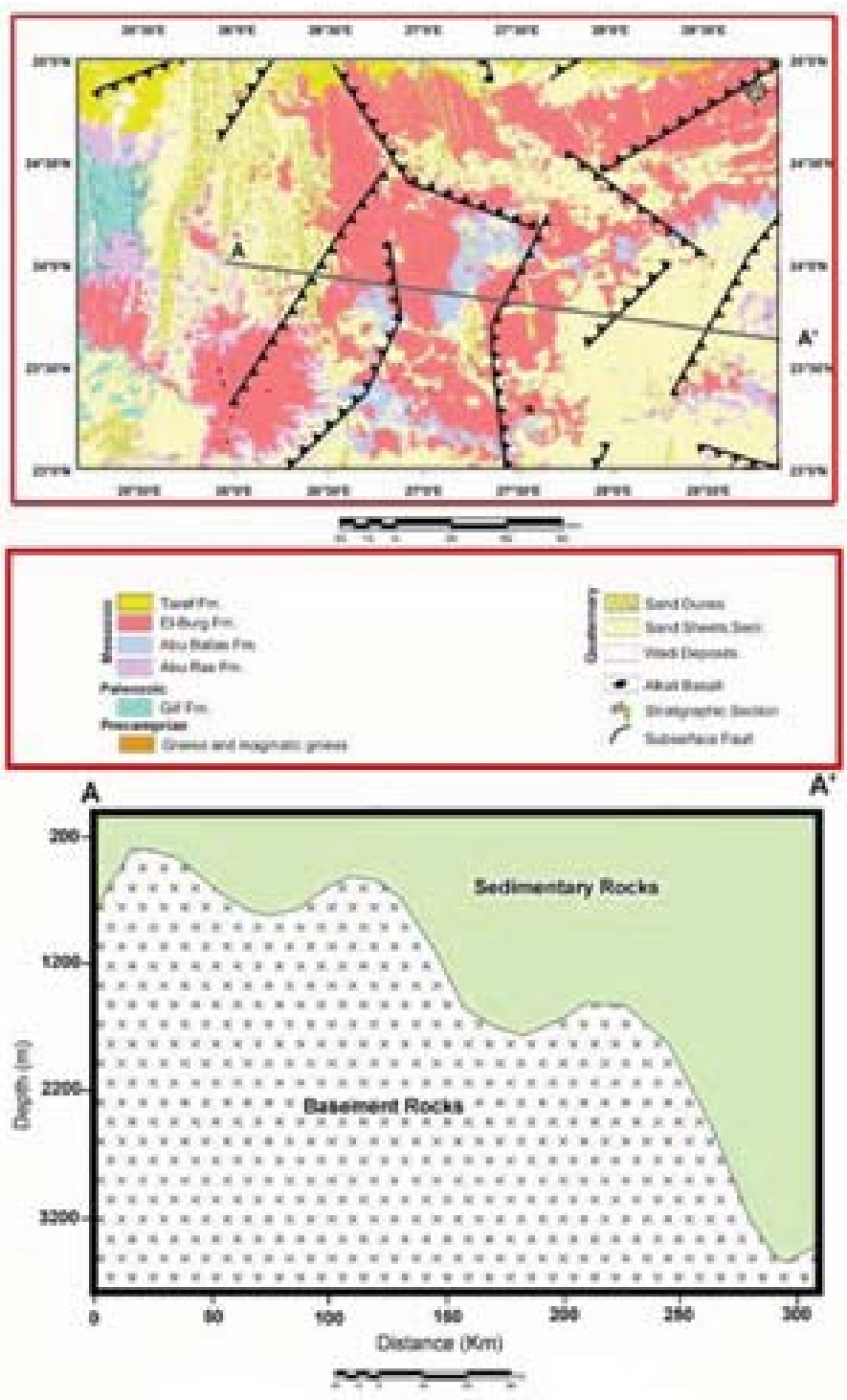

Fig. 4: Geological map for the study area.

Age	Rock unit	Lithology	Thick. (m)	Description
Quaternary				Sand sheets
				Gravels
				Chalcedony
				Playa deposits
				Volcanics
Upper Cretaceo-us	Taref Sandstone Mm.		50	Sandstone light brown to buff, highly cross bedded volcanics
Cenomenian	El Burg Fm.		111	Sandstone cross bedded, deeply weathered with kaolintic paleosoil, fossiliferous with plant remains
Permo-Triassic	Abu Ras Fm.		95	Sandstone yellowish brown cross bedded,it gets up multicolcoures fine-grained sandstone with rootled structures and koolinitic cement
Carboni-ferous	Gilf Fm.		60	Sandstone medium to coarse-grained, quartzose in parts, fossiliferous with *calamites* and *lepidosigillaria* sp
				Basement rocks

Fig. 5: Composite stratigraphic section of the study district.

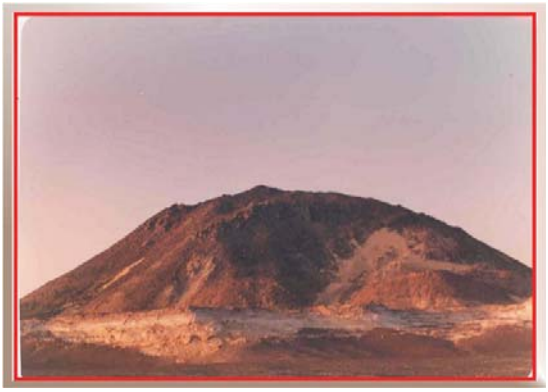

Fig. 6: Highly ferruginated beds of El Burg Formation associated with the basaltic flows at Gilf El Kebir area.

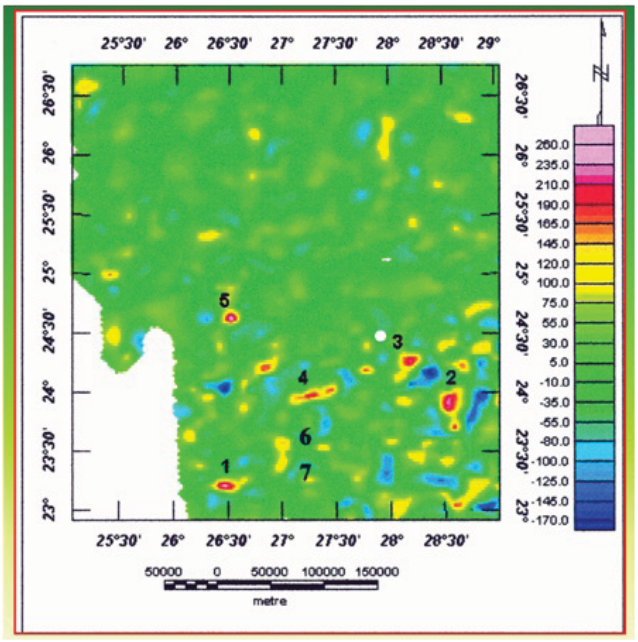

Fig. 7: Magnetic map showing the location of the magnetic anomalies, which represented the occurrences of iron deposits.

The use of density slices technique for the area of magnetic anomaly No. 4 (D3 area) produced an index map showing various degrees of ferrugination (from purple to yellow colors). In this area, the studied stratigraphic sections of Abu Ballas and El Burg formations which are cut by basaltic flows are characterized by high to moderate ferrugination. The age of both formations are Late Jurassic-Early Cretaceous and Albian-Early Cenomenian respectively. This favors that the ferrugination is stratigraphically uncontrolled and evidencing the role of basaltic flows of NE trend.

Table 1: The locations of the magnetic anomalies and their trends at the studied area

AnomalyNo.	Longitude	Latitude	Length (m)	Trend
1	26° 28' 43"	26° 28' 43"	3050	E-W
2	26° 28' 43"	26° 28' 43"	20700	N-S
3	26° 28' 43"	26° 28' 43"	19063	NE-SW
4	26° 28' 43"	26° 28' 43"	44064	NE-SW
5	26° 28' 43"	26° 28' 43"	14446	Rounded

The use of density slices technique for an area (uncovered by airborne magnetic survey) in the northern part of the Gilf El Kebir Plateau (D4, located between Lat. 23° 45' and Long 25° 45'), produced an index map showing purple to yellow colors enhancing various degrees of ferrugination. These results support that the density slices tools successfully be used in the exploration for ferruginated beds in the study district.

Results of fieldwork studies on the sites of magnetic anomalies No.1,6 &7:

Ferrugineous and manganiferous pockets and lenses were recorded nearby the basalts of the Gilf El Kebir plateau and the Black Hill area

Magnetic anomaly No. 1:

At the Gilf El Kebir plateau between Lat. 23 00' – 23 45' N and Long. 26 10' – 26 30' E, there are several localities that contain rich iron ore bands, pockets and lenses associating basaltic flows as follows:

- At the entrance of Wadi Mashi, the iron and manganese deposits are well developed associated with the basalts. The spatial association of the manganese and iron oxides with volcanic rocks suggest a hydrothermal origin, an idea suggested by Bell and Sandford (1971).
- At the area between Lat. 23° 34' 46'' N and Long. 26° 19' 082'' E, the sandstones contain 2 m thick of iron ore, very hard, reddish brown to dark brown, very dense. (Sec. G2, Fig. 8d).

The area at Lat. 23° 33' 96" N and Long. 26° 19' 67" E is highly faulted (N- S and E-W trends) and the iron ore beds reach about 3 m thick. The iron beds are present with the sandstone beds, which are highly affected by the dense faulting system (Figs. 8e and 9).

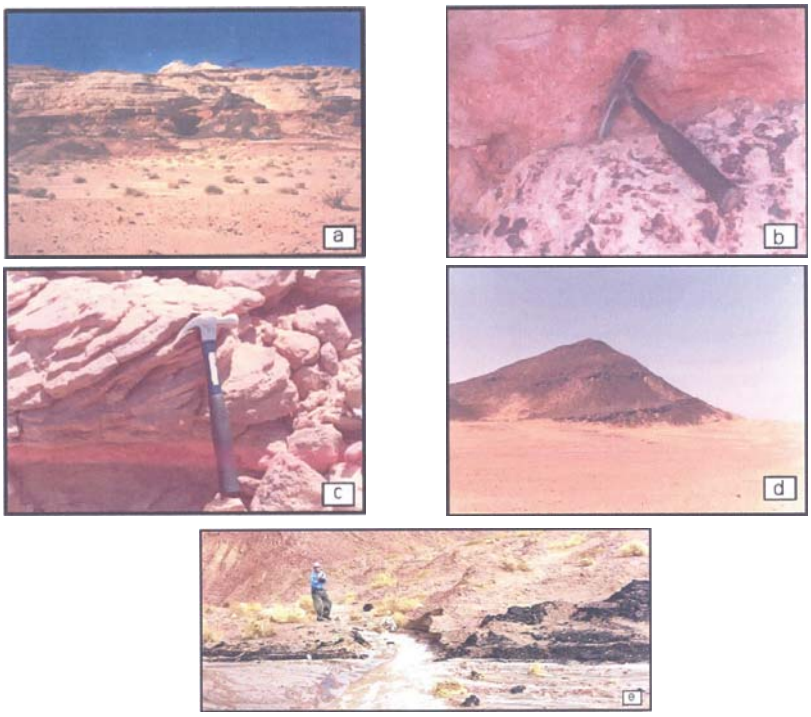

Fig.8a-8e.a: Photograph showing the Abu Ballas Formation overlain by the EI Burg Formation at central part of the sttudy district. b. Photograph showing highly ferruginated paleosle in EI Burg Formation at western part of study district. c. Photograph showing highly ferruginated beds in EI Burg Formation at eastern part of the study district. d. Photograph showing iron rich bands in EI Burg Formation near by the Black Hill area. e. Photograph showing iron rich bands in EI Burg Formation at the entrance of Wadi El Diyek.

Table 2: Chemical analysis for the ferruginated beds of theGilf El Kebir area.

Sample No.	SiO_2%	Fe_2O_3%	MnO%
1	48.7	9.3	0.05
2	47.8	10.4	0.03
3	50.6	10.6	0.08
4	46.4	10.9	0.05
6	50.7	8.4	0.3
7	47.3	10.1	0.04
8	40.3	19	0.18
9	50.6	8.1	1
10	53.8	33	0.14
11	48	13.3	0.13
12	50.6	8.6	0.02
13	47.6	11.8	0.02
14	50.4	28.6	0.3
15	59.3	1.3	0.06

- At the entrance of Wadi El Dayik (Lat. 23° 3 1' 41" N and Long. 26° 2l' 38" E), the escarpments along the wadi are mainly quartizitic sandstones with iron rich bands (1 – 2 m thick). The sandstones are cut by the basaltic sheets, which are very common in the area. The region is very dissected by different fault trends. The main trend is the E-W, while the N-S trend is also common. Moreover, 15 analyzed representative samples from the ferrugeniated beds of the Gilf El Kebir Plateau are given in table (2):

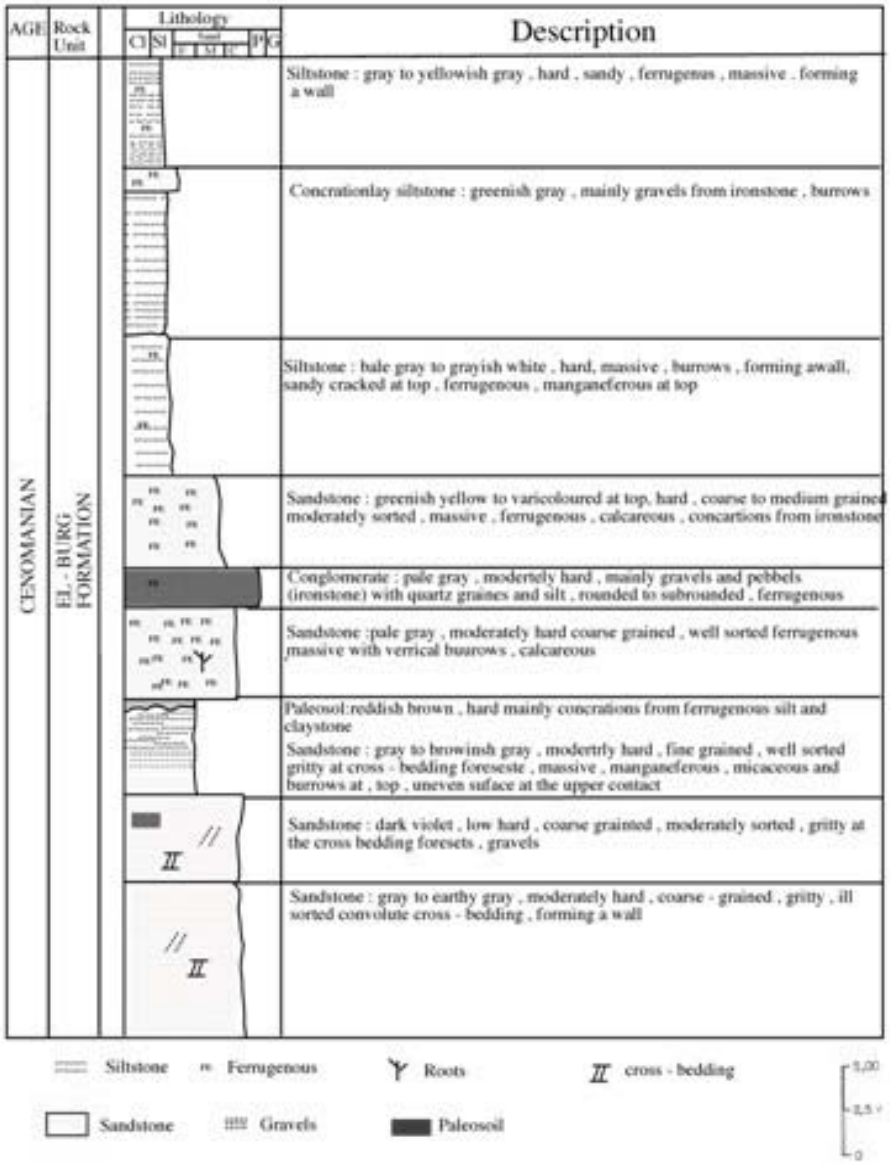

Fig. 9: Lithostratigraphic section (G2) showing the highly ferruginated beds of the El Burg Fm. at the southeastern part of the El Gilf El Kebir area.

Magnetic anomalies No. 6 & 7:

Iron and manganese deposits were also recorded in the area around the Black Hill (Long. 27° 30 and Lat. 23° 10'N, Sec. G1, Fig. 2), where extensive basaltic flows were recorded. The area of these deposits is a wide plain of about 50 km^2. Two iron ore types are recognized: i) goethite-hematite ore (50- 60 % Fe) and ii) highly ferruginated fine-grained sandstones which represent the major part of the deposit. The bands which form the iron ore strike either east - west or 70° N, and cross the sandstone country. Patches, pockets and nodular masses of rich iron oxides are common intercalations in the sandstone of this area.

Issawi (1978) analyzed three samples from the area west of the Black Hill and in which Fe_2O_3 contents range from 62.7 to 22.99 %, MnO content from 22.29 to 1 % and SiO_2 contents from 14.39 to 5.46 % .In 1981, four samples were chemically analyzed in the EGSMA Lab. derived from the Black Hill region and in which Fe_2O_3 content ranging from 79.9 to 18.59 %, Mn contents from 12 % to 0.15 % and CaO contents from 2.59 to 1.1.9 % (Dardir, 1981).

Discussion:

The stratigraphic rock formations in the study area are: the Gilf (Carboniferous), the Abu Ras (Permo-Triassic), the Abu Ballas (Late Jurassic – Early Cretaceous), and the El Burg (Albian – Early Cenomanian), along with the Taref Member (Late Cretaceous). The top beds of the Abu Ballas Formation represent the first appearance of shallow sea sediments. The top beds of El Burg Formation represents shallow marine sediments, onlapping fluviatile and deltaic sediments. The Landsat ETM+ image (band 7, 4, 2 in R, G, B) for the study area exhibited three parallel ridges trending ENE-WSW. Radarsat images revealed NE-SW subsurface fault that separated the Abu Ras from the El Gilf El Kebir Plateau and caused the ENE trend of the three ridges. This fault records continuous rejuvenation of the NE Precambrian Pleusium Megashear Zone. Also, Radarsat images enhance subsurface major fault trending NNW-SSE underneath the recent sands, east the Gilf El Kebir Plateau. This fault caused northward displacement of the three ridges.

The fieldwork study of the 22 stratigraphic sections recorded highly ferruginated beds in the El Burg Formation (Albian – Early Cenomanian) and moderate to weak ferrugination in Abu Ballas Formation. (Late Jurassic – Early Cretaceous). Some beds of the Gilf Formation (Carboniferous) and the Abu Ras Formation (Permo-Triassic) are coloured by violet to pale brown due to presence of manganese and iron oxides. In this respect, the beds of both formations in the sections located nearby the Banded Iron Formation of east Oweinat and west Gabal Kamel exhibit highly limonitic and hematitic beds.

Volcanic rocks occur in the study area. They comprise basalts, trachytes and phonolites and range in age from Carboniferous to Recent. The basalt sheets cover mainly the El Burg and occasionally the Taref formations. Also, the basaltic dykes and / or sills are trending NE-SW and NW-SE, cutting the El Burg Formation. Dykes of the highly ferruginated quartzitic sandstone, highly disturbed bedding planes and the conspicuous changes of dip of different rock units are occuring nearby these volcanic eruptions.

Most of the studied sections are located nearby the alkali basalts, occurring in fault zones of NE-SW and NW-SE trends. The variation in the ferrugination intensity is related to the sites of the ferruginated beds relative to the basaltic flows and fault zones independent on the stratigraphic position of the formations. The highest ferrugination is recorded in the NE and NW fault zones, nearby the basaltic dykes and sheets covering El Burg Formation and occasionally Taref Formation.

The magnetic map (investigated by Ramadan and Sultan, in press) integrated with the density slices tools reached to the following results: a) Grabens and horsts due to subsurface faults trending NE-SW, ENE-WSW and NW-SE. b) The intersected NW-SE, NE-SW and ENE-WSW faults, caused the apparent displacement of 3 ridges, c) The thickness of the sedimentary cover ranges from 300 m (at southwestern part of the study area) to 3400 m (at the southeastern part of the study area), d) Presence of 7 magnetic anomalies in the central part of the study area. The magnetic anomalies of Nos. 1 to 5 are strong and cover large areas, while the anomalies 6 and 7 are weak. These anomalies are located within the displaced 3 recorded ridges, e) The magnetic anomalies No.1 (Wadi El Dayik) and No. 4 (central part of the Ridge No. 2) coincide with the sites of the stratigraphic section G2 and the sections G4, G5,G6 respectively. f) The use of the density slices band ratio 3/1 reached to iron oxides index maps of the magnetic anomalies No.1, 6 and 7 which show presence of widespread purple colour reflecting high ferrugination. This ferrugination is due either to exposure of ferruginated beds by weathering or to washings of fragmented highly ferruginated beds of the Gilf El Kebir Plateau or due to both. g) The use of density slices technique for an area uncovered by airborne magnetic survey in the northern part of the Gilf El Kebir Plateau (D4, located between Lat. 23° 45' and Long 25° 45'), produced an index map showing purple to yellow colors. These results support that the density slices tools can successfully be used in the exploration for ferruginated beds in the study district.

At the Gilf El Kebir Plateau between Lat. 23 00' – 23 45' N and Long. 26 10' – 26 30' E (the magnetic anomaly No.1), there are several localities that contain rich iron ore bands, pockets and lenses. The area at Lat. 23° 33' 96" N and Long. 26° 19' 67" E is highly faulted (N- S and E-W trends) and the iron ore beds reach about 3 m thick. The Fe_2O_3 content reaches up to 28.6 % and MnO content up to 1 %. At the entrance of Wadi Mashi, the iron and manganese deposits are well developed and are associated with the basalts. At the Black Hill area (the magnetic anomalies 6 and 7), iron and manganese deposits in which Fe_2O_3 content ranges from 58.3 to 15.1 % and MnO contents from 22 % to 1 % were also recorded. The spatial association of the manganese and iron oxides with volcanic rocks suggest a hydrothermal origin.

These results support the role of the structures as well as the basaltic dykes and sheets in controlling the ferrugination intensities of the El Burg and Abu Ballas formations and occasionally El Gilf and Abu Ras formations. Moreover, the beds of these formations are intensively ferruginated in the south western part of the study area, nearby west Gabal Kamel BIF. Consequently, the role of hydrothermal activity associated with the volcanic eruptions can be suggested for the formation of ferruginated beds. The source of the iron and manganese in these hydrothermal solutions could be the fragmented BIF, accumulated chiefly in the south western part of the Dakhla Basin. This can be supported by the ideas of McCauley *et al.* (1982) who pointed out the presence of northward, westward and southward drainage in the Oweinat area till the Tertiary.

Conclusions:

All the studied sections bearing iron and iron- manganese mineralizations are located within the zone of the Pleusium Megashear System extending from Gabal Oweinat northeastward to the Baharyia Oasis. These ferruginated sections are chiefly located in the area between Lat. 23 00' – 24 30' N and Long. 25 30' – 29 30' E. This area is dissected by different faults having NE-SW (the main iron deposits), NW- SE and N-S trends. The fault trends represent extensions to those dissecting the subsurface Precambrian rocks.

The thickness of sedimentary cover ranges from 300 m to 3400 m at the south eastern part of the study area.

The stratigraphic sections of El Burg Formation (sections G1 and G2, located near alkali basalts) and the Abu Ballas Formation (sections G3, G4, G5, G6 and G8) recorded in fault zones of NE and NW trends) are including highly ferruginated beds. The ferrugination intensity of both formations is related to the fault system and not to their stratigraphic position.

All the given points of evidence probably enhance a combined action of hydrothermal solutions (accompanied basaltic eruptions) and volcanic exhalations as well as the transported weathered BIF detritus on the distribution of the iron and iron – manganese deposits.

Radarsat image revealed some subsurface features underneath the recent sands, filling the main wadis in the study area. The density slices tools (band ratio 3/1) can be successfully used in the exploration for ferruginated beds in the study district.

The density slices tools is helpful in revealing the sites of highly ferruginated beds in the studied district. This will facilitate field - work exploration.

The sites of highly ferrugination that can be recorded using density slices tool represent good targets for further detailed fieldwork and mineralogical and geochemical studies.

REFERENCES

Abdelsalam, M.G., R.J. Stern and W.G. Berhane, 2000. Mapping gossans in arid regions with Landsat TM and SIR-C/X-SAR imagery: The Boddaho alteration zone in northern Eritrea, Journal of African Earth Sciences, 30: 903-916.

Abrams, M., J. Brown, L. Lepley and R. Sadowski, 1983. Remote sensing for porphyry copper deposits in southern Arizona, Economic Geology, 78: 591-604.

Dardir, A. A., 1981. Basement rocks of the Gilf-Oweinat area. Annals Geol. Surv. Egypt, 11, 67-68.

El Ghawaby, M., 1984. Use of Landsat-images for interpretation of the geologic evolution of Gilf El Kebir area, South West Egypt. International Workshop on Remote Sensing, International Atomic Energy Agency, Vienna, 1-24.

El Kelani., 1992. Geological studies on the area between Lat. 23 – 24 30' N and Long. 29 00' – 29 30' E, southern part of the Western Desert, Egypt. M.Sc., Al Azhar Univ. Cairo, Egypt.

Hamilton and Krinsley, 1967. Upper Paleozoic glacial deposits. Geol. Soc. America Bulletin, 78, 783-800.

Hermina, M.H., M.G. Ghobrial and B. Issawi, 1961. The geology of the Dakhla area. Geol. Surv. Egypt, 33.

Issawi, B., 1969. Geology of Kurkur - Dungul area, Egypt Geol. Surv. Paper. 46: 102.

Issawi, B., 1978. New findings on the Geology of Oweinate - Gilf El kebir. Annals Geol. Surv. Egypt, 8: 275-293.

Issawi, B., 1982. Exploration of the Great Sand Sea (Abstract). Geol. Soc. America 95th Annual meeting New Orleans, U.S.A.

Issawi, *et al.*, 1996. Tectono_sedimentary synthesis of the Paleozoic basins in Egypt. Thirteen Petrol. Conf., Egypt. Gen. Petrol. Cor. Cairo., 1: 1-24.

Meneisy, M.Y. and H. Kreuzer, 1974. Potassium- Aragon ages of Egyptian basaltic rocks: Geik. Jahrbuch, 9: 21-31.

Ramadan, T.M. and A.S. Sultan, 2004. Integration of remote sensing and geophysical data for the identification of massive sulphide zones at Wadi Allaqi area, South Eastern Desert, Egypt. M.E.R.C. Ain Shams Univ., Earth Sci. Ser., 18: 165-174.

Reed, H.H. and J. Watson, 1975. Introduction to geology – Earth History. John Willey & Sons, New York, 2, 11, later stages of Earth History, 371.

Sahins, F.F., 1997. Remote Sensing Principles and Interpretation, W.H. Freeman and Company, New York, 494.

Sultan, M., R.E. Arvidson and N.C. Sturchio, 1986. Mapping of ser-pentinites in the Eastern Desert of Egypt by using Landsat Thematic Mapper data, Geology, 14: 995-999.

Sultan, M., R.E. Arvidson, N.C. Sturchio and E.A. Guiness, 1987. Lithologic mapping in arid regions with Landsat Thematic Mapper data: Meatiq dome, Egypt, Geological Society of America Bulletin, 99: 748-762.